

# Synthesis of Polymeric Flame Retardants Containing Phosphorus-Nitrogen-Bromide and Their Application in Acrylonitrile-Butadiene-Styrene

Li Yan,<sup>1</sup> Yubin Zheng,<sup>1,2</sup> Jianping Liu,<sup>1,3</sup> Hongzhou Shang<sup>1</sup>

<sup>1</sup>Department of Polymer Science and Materials, Dalian University of Technology, Dalian 116012, People's Republic of China

<sup>2</sup>State Key Laboratory of Fine Chemicals, Dalian University of Technology, Dalian 116012, People's Republic of China

<sup>3</sup>College of Chemistry and Materials Engineering, Wenzhou University, Wenzhou 325027, People's Republic of China

Received 20 December 2008; accepted 17 June 2009

DOI 10.1002/app.30972

Published online 15 September 2009 in Wiley InterScience (www.interscience.wiley.com).

**ABSTRACT:** A series of polymeric flame retardants (PFRs) containing phosphorus-nitrogen-bromide were synthesized from spirocyclic pentaerythritol bisphosphate disphosphoryl chloride (SPDPC), 2-methoxyl-4,6-dichloro-1,3,5-triazine (MDCT), and tetrabromobisphenol A (TBBPA). The influence of monomer ratio on their thermal stability was investigated by adjusting the proportion of SPDPC/MDCT (mol/mol) from 80/20 to 20/80. The flammability properties of the PFRs blended with ABS were evaluated using LOI and UL-94 vertical test. The structures of the flame retardants were characterized by means of Fourier transform infrared spectra

(FTIR) and proton nuclear magnetic resonance spectroscopy (<sup>1</sup>H-NMR). The results show that the initial temperature of decomposition is 274°C and with 35% charring residue at 500°C when the ratio of SPDPC/MDCT is 50/50. V-0 ratings in the UL-94 vertical test were achieved at 20–30% loading of PFRs, when LOI values reached at least 26.9%. The flame retardancy is strongly dependent on the ratio of P, N, and Br. © 2009 Wiley Periodicals, Inc. *J Appl Polym Sci* 115: 957–962, 2010

**Key words:** synthesis; flame retardance; spirocyclic pentaerythritol bisphosphate; ABS; TGA

## INTRODUCTION

Acrylonitrile-butadiene-styrene (ABS) is often used as electronic devices. In most fields, it has to meet high-flame retardancy standards.<sup>1–3</sup> However, ABS is extremely flammable and generates heavy black smoke. The traditional flame retardants used in ABS are decabromodiphenyl oxide (DBDPO) and antimony trioxide (Sb<sub>2</sub>O<sub>3</sub>) which have been recognized to be harmful to the environment.

Nowadays, phosphorus-containing flame retardants have been developed to replace DBDPO,<sup>4</sup> such as triphenyl phosphate (TPP) and resorcinol bis(diphenyl phosphate) (RDP),<sup>5–7</sup> however, Levchik and Weil have clearly stated in their excellent review article that a single phosphorus-based flame retardant is difficult to give UL-94 V-0 rate for styrenic plastics including ABS.<sup>4</sup> Introducing a char-forming additive into phosphate flame retarding ABS is an effective method to obtain flame retardancy, such as novolac phenol resins reported in Bae's articles<sup>8–10</sup> and cyclic phosphonates reported by Hoang<sup>10</sup> and Ma.<sup>3</sup> With about 30 wt % loading of these halogen-

free flame retardants, the LOI could reach to about 28%. In all the composites, the phosphorus content of the char was substantial. This is characteristic of the condensed-phase flame retardant action of phosphorus enhanced by char formers. The char-forming components involve spirocyclic pentaerythritol bisphosphate structure and triazine derivatives as well.<sup>11–19</sup> But it may suffer from a cost disadvantage when compared with organobromine ones. If flame retardants would promote char formation at the surface of the polymer and display effective gas-phase disruption of combustion simultaneously, an efficient flame retardant for ABS might be possible. Introducing phosphorus, nitrogen, or other elements which are known to enhance char formation at the surface of burning polymers into the bromine-containing molecule might generate both the good gas-phase and condensed-phase activity.<sup>20</sup> In fact, some of them have been proved to display a synergy action.<sup>21–23</sup> For example, only 5 wt % loading of (2,4,6-tribromophenyl) diethylphosphate in polystyrene could pass the UL-94 test V-0 rating.<sup>20</sup> It should cut down the cost required to achieve an acceptable level of flammability and reduce the potential environmental effect.

On the other hand, compared with small flame retardants, polymeric flame retardants (PFRs) have

Correspondence to: Y. Zheng (zybwl@163.com).

TABLE I  
The Effect of SPDPC/MDCT on  $\eta_{inh}$

Flame retardants	$\eta_{inh}^a$ dL/g	SPDPC/MDCT		P % in PFRN	% in PFRBr	% in PFR
		Calcd.	Analy. <sup>b</sup>			
PFR28	0.08	20/80	22/78	1.8	5.0	47.5
PFR55	0.10	50/50	51/49	4.4	3.0	45.1
PFR73	0.11	70/30	71/29	5.9	1.7	43.7
PFR82	0.12	80/20	82/18	6.7	1.1	43.0

<sup>a</sup> C = 0.5 g/dL, in a DMF solution at 30°C.

$$^b \text{SPDPC/MDCT} = \frac{\sum_{4.5 \text{ ppm}}^{5.0 \text{ ppm}} \mathbf{H} / 8}{\sum_{3.8 \text{ ppm}} \mathbf{H} / 3}$$

been applied for their higher thermal stability and better resistance to migration and volatile loss. In addition, Ma et al.<sup>3</sup> had synthesized an oligomer to improve the evaporation temperature. Wang et al.<sup>23–25</sup> had synthesized several oligomeric phosphates which could reduce the adverse effect on mechanical properties.

Encouraged by these studies, a series of PFRs containing phosphorus, nitrogen and bromine have been synthesized in our works. We introduced phosphorus as acid source, pentaerythritol and triazine as char former to carry out condensed-phase action and introduced bromine to utilize the synergistic effect between condensed-phase and gas-phase. The influence of monomer ratio on their thermal stability was investigated by adjusting the proportion of spirocyclic pentaerythritol bisphosphorate disphosphoryl chloride (SPDPC) and 2-methoxy-4,6-dichloro-1,3,5-triazine (MDCT). Furthermore, the thermal decomposition property of the optimal flame-retarded composites was investigated. The mechanical properties of the flame-retarded composites were tested.

## EXPERIMENTAL

### Materials

Unless otherwise stated, all materials were obtained from commercial suppliers and used without further purification. The ABS resin (750A) was purchased from Daqing Petrification Factory, P.R.China. Pentaerythritol of C.R. grade was purchased from Shanghai Lingfeng Chemical Plant. Spirocyclic pentaerythritol bisphosphorate disphosphoryl chloride (SPDPC) was synthesized via the method suggested by Rudi.<sup>26</sup> 2-methoxy-4,6-dichloro-1,3,5-triazine (MDCT) was prepared according to the reference.<sup>27</sup> Tetrabromobisphenol A (TBBPA) of A.R. grade was purchased from Dead Sea Bromine Group, Israel. Decabromodiphenyl oxide (DBDPO) and antimony trioxide ( $\text{Sb}_2\text{O}_3$ ) were purchased from Guoyao Group of chemical reagents (Shenyang, China).

### Synthesis of PFRs

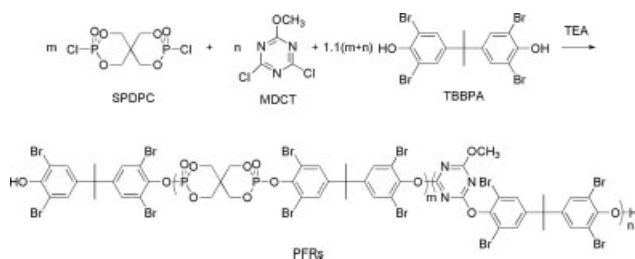
The PFRs were synthesized via nucleophilic substituent reaction. In a clean, dry 250 mL flask, TBBPA 59.8 g (0.11 mol) was dispersed in acetonitrile (150 mL). Subsequently, a mixture of SPDPC and MDCT in a calculated molar ratio (Table I) was added. The mixture was stirred and triethylamine 22.2 g (0.22 mol) was added dropwise for 2 h at room temperature. Whereafter, the mixture was gradually heated under nitrogen. The reaction would be completed after 6 h at 80°C. The white powder was filtered and purified with water and then dried to constant weight at 100°C in vacuum oven. The product was obtained in the yield of 97.3–98.2%.

### Preparation of flame-retardant ABS resins

All the components were dried in a vacuum oven at 100°C for 8 h. ABS resins containing different PFR with different content were prepared via melt compounding at 200°C in ThermoHaake rheomixer with a rotation speed of 40 rpm for 10 min. The samples were transferred to a mold and preheated at 200°C for 15 min. Then, the samples were pressed at 10 MPa and cooled to room temperature with the retaining pressure. The composite resins were  $100 \times 6.5 \times 3 \text{ mm}^3$  and  $100 \times 12.5 \times 3.2 \text{ mm}^3$  sheets for LOI and UL-94V tests, respectively.

### Measurements

Inherent viscosities (IV) of the PFRs were measured in a DMF solution at 30°C with the PFR concentration of 0.5 g/dL by an Ubbelohde viscometer. Melting points were determined by TX-4 melting instrumentation. The Fourier transform infrared (FTIR) spectra (in KBr pellets) were recorded by a Nicolet 20DXB FTIR spectrophotometer. The <sup>1</sup>H-NMR spectra were obtained at 25°C in DMSO-d<sub>6</sub> using a Bruker Advance II 400 MHz NMR Spectrometer with TMS as the internal standard. Thermo



**Scheme 1** The synthesis of PFRs.

gravimetric analysis (TGA) was completed by the TGA/SDTA851<sup>®</sup> thermal analyzer at a scanning rate of 10°C/min under nitrogen atmosphere from 50 to 500°C. LOI test was performed according to the test procedure of ISO4589-1984. UL-94 V test was conducted on a CZF-2 instrument.

## RESULTS AND DISCUSSION

### Synthesis of PFRs

The synthesis route of PFRs was shown in Scheme 1. The content of SPDPC/MDCT (mol/mol) was controlled at 80/20(PFR82), 70/30(PFR73), 50/50(PFR55), and 20/80(PFR28). To improve the thermal properties of the products, we adjusted the Br, N, and P content.

The FTIR and <sup>1</sup>H-NMR spectra of PFRs were almost identical and differed only in relative signal intensities. In the FTIR spectrum of PFR55, (Fig. 1) the new stretching vibration peaks of P—O—C(Φ) and C—O—C(Φ) appear at 935, 1284 cm<sup>-1</sup>, accompanying the vanishing of P—Cl and C—Cl stretching vibrations at 547 and 542 cm<sup>-1</sup> peaks. It indicates the completion of polymerization. The chemical structures and the unit ratio of PFRs were further confirmed by <sup>1</sup>H-NMR spectra. The typical <sup>1</sup>H-NMR spectrum of PFR55 is shown in Figure 2. Here, the

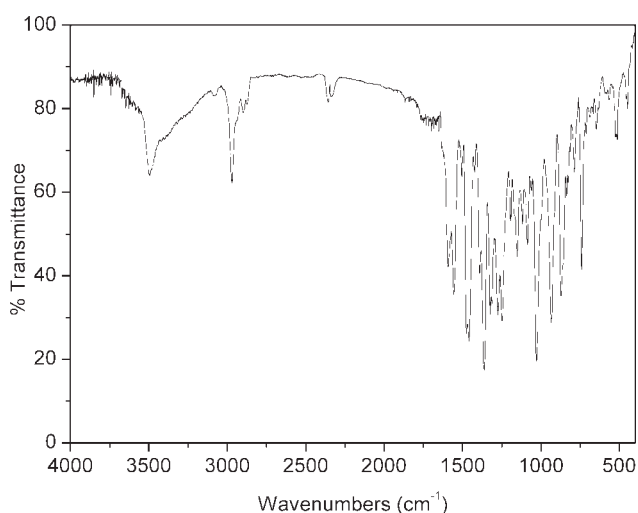


**Figure 1** FTIR spectrum of PFR55.

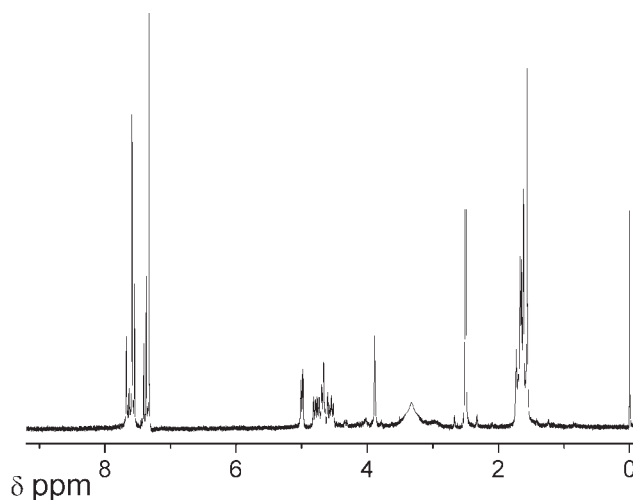


**Figure 2** <sup>1</sup>H-NMR spectrum of PFR55.

peak of H: 4.52–4.98 ppm (8H—CCH<sub>2</sub>O—PO—) confirms the structure of SPDPC, 3.88 ppm (3H, —OCH<sub>3</sub>) confirms the structure of MDCT. So the ratio of SPDPC/MDCT of oligomer composition can be calculated via <sup>1</sup>H-NMR spectra data. The determined data of SPDPC/MDCT in detailed is listed in Table I. Owing to the higher reaction ability of SPDPC with TBBPA, the reaction degree of SPDPC is higher than MDCT in the same reaction time. So the inherent viscosities of PFRs increased with the increasing of SPDPC unit (Table I).

### Thermal stability of PFRs

Figure 3 shows the initial decomposition temperature (5% weight-loss) of PFRs is at 274–321°C and the residues at 500°C under nitrogen are over 30%. The plentiful char residue indicates that PFRs are

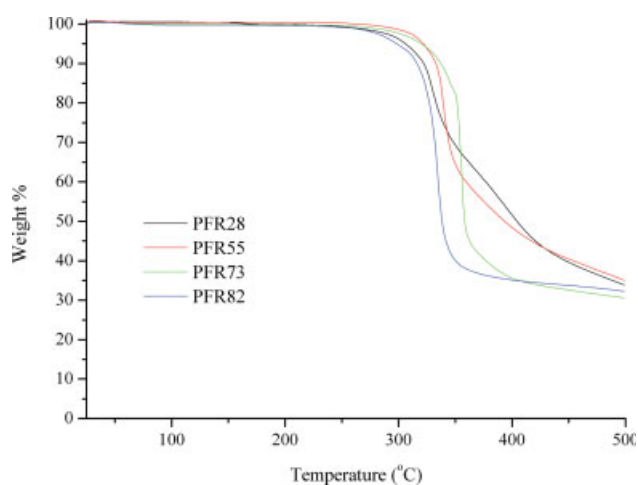


**Figure 3** TGA curves of PFRs at a heating rate of 10°C/min under N<sub>2</sub> atmosphere. [Color figure can be viewed in the online issue, which is available at [www.interscience.wiley.com](http://www.interscience.wiley.com).]

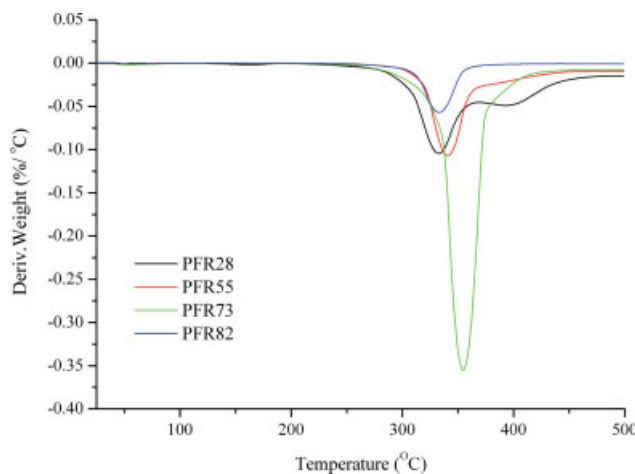


**Figure 4** DTG curves of PFRs at a heating rate of 10°C/min under N<sub>2</sub> atmosphere. [Color figure can be viewed in the online issue, which is available at [www.interscience.wiley.com](http://www.interscience.wiley.com).]

efficient char formers and they might generate the protective char layer on the surface of the burning polymers. On the other hand, the sufficient thermal stability of PFRs can meet the processing temperature of ABS. DTG results indicates that PFRs have a major weight-loss stage from 280 to 400°C, (Fig. 4), assigned by the degradation of organic bromine and the scission of the phosphate ester bonds synchronously. The onset decomposing temperature and the residues show irregularly at the monomer ratio. Moreover, the degradation stages of PFRs are various from different ratio of SPDPC and MDCT in the structures. With the increase of SPDPC, the compounds decompose rapidly and the TGA curves show weight-loss sharply. On the contrary, with the increase of MDCT, the TGA curves become flat, which is due to the higher thermal stability of triazine structure. Compared with the TGA curve of pure ABS (Fig. 5), the PFRs' thermal decomposition behaviors match with ABS, especially PFR55. When PFR loses about 50% weight, pure ABS starts decomposing. The proper gap of initial degradation temperature between the polymer and flame retardant is necessary for producing phosphoric acid and emitting bromine at the beginning of combustion.

### Flammability properties

The PFRs have been added in ABS and their flammability was evaluated by LOI and UL-94 vertical test. The results are listed in Table II. From UL-94 test, V-0 rating is achieved at 20–30 wt % loading of PFRs for ABS (except for PFR28). With the increase of PFRs, the LOI of compositions increases from 18.1 to 27.6.

The flame retarding effect is due to the gas-phase action from bromine and condensed-phase action

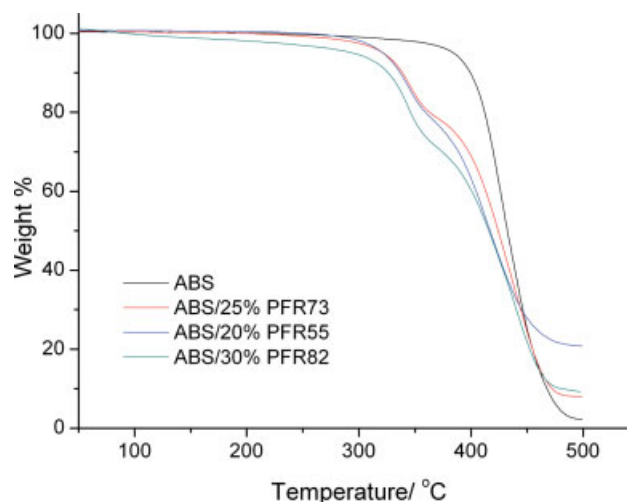


**Figure 5** TGA curves of pure ABS and flame-retarded ABS at a heating rate of 10°C/min under N<sub>2</sub> atmosphere. [Color figure can be viewed in the online issue, which is available at [www.interscience.wiley.com](http://www.interscience.wiley.com).]

from nitrogen and phosphorus. Because the Br contents of PFRs are not much different (Table I), the flame retarding action is strongly depends on the mol ratio of N/P in flame retardants. Although the flame retarding effect becomes manifest with increase of the N/P mol ratio in PFRs, when the ratio of element N/P reaches to 6/1 (PFR28), the LOI values decrease quickly. Increasing the ratio of N/P does not always mean better condensed-phase action. In other words, there exists a distinct synergistic effect (SE) between element N and P. So proper ratio of N/P can promote char formation at the surface of the polymer and present condensed-phase flame retarding action. It is concluded that the good condensed-phase flame retarding action is helpful to promote the efficiency of PFRs. Therefore, PFR55 displays the optimal result, which disrupts combustion in the gas-phase and at the same time promotes char formation at the surface of polymer.

**TABLE II**  
Results of LOI Measurements and UL-94 Combustion Test

Entry	N/P ratio in PFR (mol/mol)	Sample (wt ratio)	LOI%	UL-94
0		ABS	18.1	
1	6/1	ABS/PFR28(80/20)	23.7	V-1
2		ABS/PFR28(70/30)	24.1	V-1
3	1.5/1	ABS/PFR55(80/20)	27.1	V-0
4		ABS/PFR55(75/25)	27.6	V-0
5	0.6/1	ABS/PFR73(80/20)	26.8	V-1
6		ABS/PFR73(75/25)	27.2	V-0
7	0.4/1	ABS/PFR82(80/20)	23.2	V-1
8		ABS/PFR82(75/25)	25.4	V-1
9		ABS/PFR82(70/30)	26.9	V-0

**TABLE III**  
Data of TGA and DTG Curves for ABS and Flame-Retarded Composites under N<sub>2</sub> Atmosphere at a Heating Rate of 10°C/min

Sample	$T_{\text{onset}}$ (°C)	Residue at 500°C (%)	$T_{\text{max}}$ (°C)	
			Stage 1	Stage 2
ABS	385	2.0		430
ABS/25%PFR73	322	8.0	344	437
ABS/20%PFR55	321	20.7	344	418
ABS/30%PFR82	297	9.4	344	417

$T_{\text{onset}}$ , initial decomposition temperature of 5% weight-loss;  $T_{\text{max}}$ , maximum weight-loss temperature.

### Thermal stability of flame-retarded ABS composites

TGA curves of flame-retarded ABS offer much information about their thermal stability and thermal degradation behavior. The detail data such as initial decomposition temperature ( $T_{\text{onset}}$ ) and maximum weight-loss rate temperature ( $T_{\text{max}}$ ) for these flame-retarded systems and ABS are listed in Table III. Figures 5 and 6 show that the decomposition mechanism of ABS is changed by PFRs. There is only one-step decomposition from 350 to 480°C of ABS, whereas flame-retarded ABS composites show two-step decomposition (Fig. 5). The first step of flame-retarded ABS is due to the decomposition of PFRs at relatively low temperature, forming phosphorus-rich char layer on the surface of polymer and the bromine-rich layer in gas phase. This can limit the production of combustible gases by cross-linking reaction<sup>20,28</sup> and protect the polymer in gas phase by reducing free radical. The residue of flame-retarded ABS is improved by PFRs as well. DTG curves (Fig. 6) show that the weight-loss speed of flame-retarded ABS is much slower than that of pure ABS in the second degradation stage. It can be concluded that the addition of PFRs can enhance the thermal stability at high temperature although it reduces the initial decomposition temperature. On the other hand, it is proposed that the char residue on pyrolysis is linearly proportional to oxygen index.<sup>29</sup> The

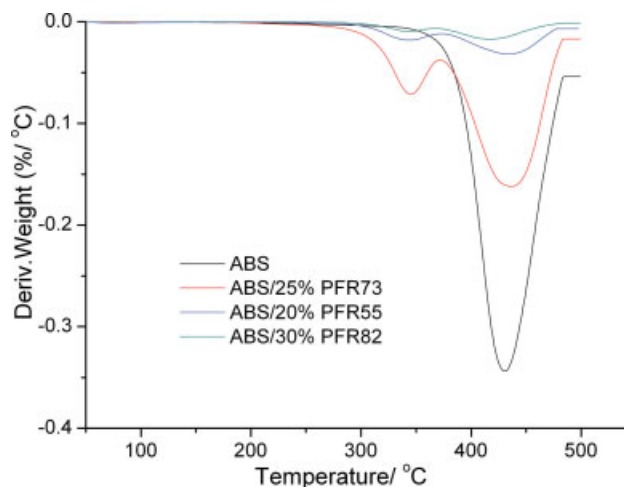


**Figure 6** DTG curves of pure ABS and flame-retarded ABS at a heating rate of 10°C/min under N<sub>2</sub> atmosphere. [Color figure can be viewed in the online issue, which is available at [www.interscience.wiley.com](http://www.interscience.wiley.com).]

substantial char residue of PFR55 is the characteristic of the condensed phase flame retardant action.

### Mechanical properties of flame-retarded ABS composites

As is known, incorporating flame retardants into ABS displays obvious disadvantages, especially, a great loss of the mechanical properties. We can see in Table IV, compared with pure ABS, flame-retarded composites samples containing PFRs have noticeable change in mechanical properties. Compared with the traditional system of DBDPO and Sb<sub>2</sub>O<sub>3</sub>, the impact strength improves partly. It is due to the better compatibility of PFRs in ABS and absence of Sb<sub>2</sub>O<sub>3</sub>. It is obvious that the study should be focused on improving the mechanical properties of the flame-retarded ABS in the future.

## CONCLUSIONS

The novel oligomeric flame retardants containing phosphorus, nitrogen, and bromine were synthesized

**TABLE IV**  
Mechanical Properties of Flame-Retarded ABS Composites

Sample (wt ratio)	Tensile strength (Mpa)	Elongation at break (%)	Impact strength (kJ/m <sup>2</sup> )	Flexural strength (Mpa)
ABS	46.7	20.2	15.9	65.0
ABS/PFR55(80/20)	45.9	11.0	9.9	65.7
ABS/PFR55(75/25)	45.6	9.8	9.4	66.3
ABS/PFR73(75/25)	44.3	9.3	9.1	66.5
ABS/PFR73(70/30)	43.9	9.1	8.9	67.1
ABS/PFR82(70/30)	44.2	8.4	8.1	67.4
ABS/DBDPO/ Sb <sub>2</sub> O <sub>3</sub> (78/18/4)	39.3	5.2	6.1	68.9

successfully. The PFRs exists a distinct synergistic effect (SE) between element N and P. PFR55 displays the optimal flame retarding action, which disrupts combustion in the gas-phase and at the same time promotes char formation on the surface of polymer. V-0 ratings in the UL-94 vertical test were achieved at 20–30% loading of PFRs, when LOI values reached at least 26.9% (Table II). It is a potential flame retardant for other polymer systems containing no char-forming component. While, the study should be focused on improving the mechanical properties of the flame-retarded ABS based on PFR55 in the future.

## References

1. Pawlowski, K. H.; Scharrel, B. *Polym Int* 2007, 56, 1404.
2. Owen, S. R.; Harper, J. F. *Polym Degrad Stab* 1999, 64, 449.
3. Ma, H. Y.; Tong, L. F.; Xu, Z. B.; Fang, Z. P.; Jin, Y. M.; Lu, F. Z. *Polym Degrad Stab* 2007, 92, 720.
4. Levchik, S. V.; Weil, E. D. *Polym Int* 2008, 57, 431.
5. Kim, J.; Lee, K.; Bae, J.; Yang, J.; Hong, S. *Polym Degrad Stab* 2003, 79, 201.
6. Lee, K.; Kim, J.; Bae, J.; Yang, J.; Hong, S.; Kim, H. K. *Polymer* 2002, 43, 2249.
7. Costa, L.; Montelera, L. R. D.; Camino, G.; Weil, E. D.; Pearce, E. M. *J Appl Polym Sci* 1998, 68, 1067.
8. Ji, Y.; Kim, J.; Bae, J. Y. *J Appl Polym Sci* 2006, 102, 721.
9. Seo, K.; Kim, J.; Bae, J. Y. *Polym Degrad Stab* 2006, 91, 1513.
10. Hoang, D. Q.; Kim, J.; Jang, B. N. *Polym Degrad Stab* 2008, 93, 2042.
11. Chen, G. H.; Yang, B.; Wang, Y. Z. *J Appl Polym Sci* 2006, 102, 4978.
12. Chen, D. Q.; Wang, Y. Z.; Hu, X. P.; Wang, D. Y.; Qu, M. H.; Yang, B. *Polym Degrad Stab* 2005, 88, 349.
13. Allen, D. W.; Anderton, E. C.; Bradley, C. *Polym Degrad Stab* 1995, 47, 67.
14. Gao, F.; Tong, L. F.; Fang, Z. P. *Polym Degrad Stab* 2006, 91, 1295.
15. Hu, X. P.; Li, W. Y.; Wang, Y. Z. *J Appl Polym Sci* 2004, 94, 1556.
16. Li, B.; Xu, M. J. *Polym Degrad Stab* 2006, 91, 1380.
17. Mahapatra, S. S.; Karak, N. *Polym Degrad Stab* 2007, 92, 947.
18. Wu, B.; Wang, Y. Z.; Wang, X. L. et al. *Polym Degrad Stab* 2002, 76, 401.
19. Chen, Y.; Wang, Q. *Polym Degrad Stab* 2007, 92, 280.
20. Howell, B. A. *Polym Degrad Stab* 2008, 93, 2052.
21. Green, J. J. *Fire Sci* 1994, 12, 257.
22. Green, J. J. *Fire Sci* 1994, 12, 338.
23. Ban, D. M.; Wang, Y. Z.; Yang, B. *Eur Polym J* 2004, 40, 1909.
24. Chang, Y. L.; Wang, Y. Z.; Ban, D. M. *Macromol Mater Eng* 2004, 289, 703.
25. Wang, D. Y.; Ge, X. G.; Wang, Y. Z.; Wang, C.; Qu, M. H.; Zhou, Q. *Macromol Mater Eng* 2006, 291, 638.
26. Rätz, R.; Sweeting, O. J. *J Org Chem* 1963, 28, 1612.
27. Thurston, J. T. *J Am Chem Soc* 1951, 73, 2986.
28. Lu, S. Y.; Hamerton, I. *Prog Polym Sci* 2002, 27, 1661.
29. Krevelen, D. W. *Polymer* 1975, 16, 615.